CHEMISTRY
A European Journal

A Journal of
ChemPubSoc Europe

Accepted Article

Title: Synthesis and Photophysical Characterization of 2,3-Dihydroquinolin-4-imines: New Fluorophores with Color-Tailored Emission

Authors: Chih-Hung Chou, Basker Rajagopal, Chien-Fu Liang, Kuan-Lin Chen, Dun-Yuan Jin, Hsing-Yin Chen, Hsiu-Chung Tu, Yo-Ying Shen, and Po-Chiao Lin

To be cited as: *Chem. Eur. J.* 10.1002/chem.201703998

Link to VoR: http://dx.doi.org/10.1002/chem.201703998

Supported by
ACES

WILEY-VCH

10.1002/chem.201703998

WILEY-VCH

Synthesis and Photophysical Characterization of 2,3-Dihydroquinolin-4-imines: New Fluorophores with Color-Tailored Emission

Chih-Hung Chou,[+,a] Basker Rajagopal,[+,a] Chien-Fu Liang,[b] Kuan-Lin Chen,[a] Dun-Yuan Jin,[a] Hsing-Yin Chen,[*c] Hsiu-Chung Tu,[a] Yu-Ying Shen,[a] and Po-Chiao Lin[*a]

Abstract: In this study, a series of variously substituted 2,3-dihydroquinolin-4-imines (DQIs) were synthesized from *N*-substituted propargylanilines by copper(I)-catalyzed annulation. The approach adopted in this study under mild, effective conditions exhibited broad substrate tolerance, particularly for functional groups substituted on anilines. Most of the DQI derivatives synthesized under optimal conditions were obtained in good isolated yields of 63–88%. 2,3-Dihydroquinolinimine thus obtained was easily converted to important structures like 2,3-dihydroquinolone and tetrahydrobenzodiazepin-5-one, confirming the importance of this strategy in constructing various heterocycles. Surprisingly, 2,3-dihydroquinolinimines thus obtained exhibited bright fluorescence with quantum yields up to 66%. The density functional theory (DFT) and time-dependent DFT (TD-DFT) calculations were performed for understanding the excited-state nature of DQI system. Accordingly, a tailored DQI derivative bearing methoxy group at C-6 position and acetoxy group at C-7 position was designed and synthesized to give emission at 559 nm with red-shift compared to the 7-methoxy substituted DQI. A detailed study of DQI structures with their photophysical properties was performed with five control molecules and consequently demonstrated the uniqueness of the chemical structures of DQIs.

Introduction

The development of effective synthetic methodologies for preparing alkaloids owing to their ubiquitous presence in natural products, pharmaceuticals, and material chemistry is of great interest for modern organic chemistry.[1] Since the early 1960s, quinolone and its analogs have been considered ideal antibiotics, attributed to their high potency and low incidence of side effects.[2a-b] In addition, its reduced form, 2,3-dihydroquinolinone, is an important privileged structural subunit found in a number of bioactive small molecules. For instance, 2,3-dihydroquinolinone is found in the acronycine family of alkaloids, exhibiting potent anti-cancer properties,[3] as antagonists of the CRTH2 receptor,[4] and in several antitumor and antimitotic agents.[5] However, only a few methods have been reported for the preparation of 2,3-dihydroquinolone, limiting the prospects for extensive study of these compounds. Typically, corrosive reagents like orthophosphoric acid, acetic acid, or strong alkalis have been used for catalyzing the isomerization of substituted 2-aminochalcones to 2,3-dihydroquinolones, which possibly limits the substrate scope considerably (Scheme 1 (a)).[6a-f] Recently, intramolecular cyclization under milder conditions using transition metal catalysts or organocatalysts have emerged as important strategies. Sierra and co-workers have reported the Pd-catalyzed synthesis of 2,3-dihydroquinolinones from (2-iodoanilino)-aldehydes (Scheme 1(b)).[7] Lu and co-workers have reported the asymmetric synthesis of 2-aryl-2,3-dihydro-4(1*H*)-quinolinones using a chiral tertiary amine tethered to a bifunctional thiourea derivative (Scheme 1(c)).[8] Bunce and co-workers have reported a strategy for the synthesis of substituted 2,3-dihydro-4(1*H*)-quinolinones by the addition of an imine via the S_NAr approach (Scheme 1(d)).[9] As shown in Scheme 1, all the above-mentioned methods have utilized suitable ortho substituents of anilines or fluorobenzene for participating in cyclization. The preparation of the starting disubstituted benzenes is tedious and time-consuming. Hence, there is an emerging need for new synthetic strategies from easily accessible starting compounds, which affords diverse range of these molecules.

To this end, we reported a simple methodology for preparing 2,3-dihydroquinolin-4-imine (DQI) from aniline-tethered *N*-sulfonyltriazole by thermal-assisted denitrogenative annulation [Scheme 1 (e)].[10] The DQIs thus obtained could be easily transformed to various 2,3-dihydroquinolones. This metal-free approach involves the decomposition of *N*-sulfonyltriazoles into a ketenimine intermediate by the heat obtained from the release of nitrogen, followed by the intramolecular trapping of the electrophilic ketenimine intermediate by the aryl ring. As the thermal reaction is significantly promoted by the presence of electron-donating groups (EDGs) at the meta position of anilines, the substrate scope is restricted, considerably limiting its use.[10] For expanding the substrate scope under milder conditions, instead of with thermal activation, transition-metal catalysis can be employed for constructing DQIs, which might overcome the need for the electron-donating effect. In 2005, Chang and co-

[a] [+]Chih-Hung Chou, [+]Basker Rajagopal, Kuan-Lin Chen, Dun-Yuan Jin, Hsiu-Chung Tu, Yu-Ying Shen, Prof. Po-Chiao Lin
Department of Chemistry, National Sun Yat-sen University
70 Lienhai Rd., Kaohsiung 80424, Taiwan
E-mail: pclin@mail.nsysu.edu.tw
[b] Prof. Chien-Fu Liang
Department of Chemistry, National Chung-Hsing University
145 Xingda Rd., South Dist., Taichung City 402, Taiwan
[c] Prof. Hsing-Yin Chen
Department of Medicinal and Applied Chemistry, Kaohsiung Medical University
100,Shih-Chuan 1st Road,Kaohsiung,80708,Taiwan
E-mail: hychen@kmu.edu.tw
+ Chih-Hung Chou and Basker Rajagopal are in equal contribution.

Supporting information for this article is given via a link at the end of the document.

10.1002/chem.201703998

workers have reported a highly efficient copper-catalyzed multicomponent strategy, in which sulfonyl azides react with a wide range of alkynes and amines to form amidines.[11] This reaction forms a highly reactive ketenimine intermediate that can be trapped with various nucleophiles and subsequently used for synthesizing various important heterocyclic structures[12] like 4-sulfonamidoquinolines,[13] 1,2-dihydroisoquinolines,[14] 3-aminopyrazoles,[15] indolines,[16] fused indolines,[17] and 2-imino-3-pyrrolines.[18] Inspired by this ketenimine chemistry, we have reported an easier route to dihydropyrimidin-4-ones and β- and β^3-amino acid analogs from propargylamides using this reactive

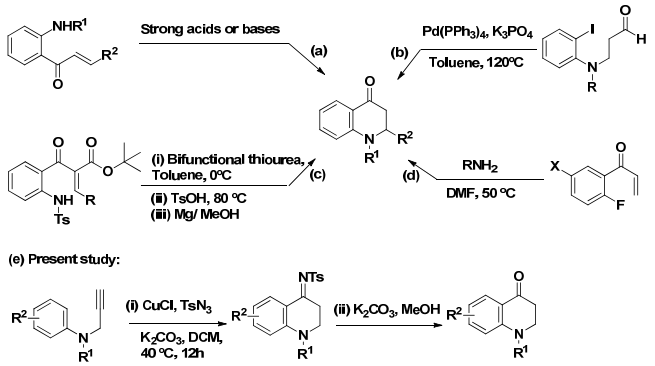

ketenimine intermediate by an intramolecular synthetic strategy.[19]

Scheme 1. Preparation of 2,3-dihydro-4-quinolones from reported methods and our recent study

Based on this easily accessible method, the Cu(I)-catalyzed denitrogenative annulation of *N*-propargylanilines using a copper(I) catalyst is proposed for facilitating a series of DQIs, as shown in Scheme 1e. The desired 2,3-dihydroquinolones were then easily obtained by basic hydrolysis. The coupling of sulfonyl azide and terminal alkyne using a simple copper(I) catalyst into the ketenimine intermediate exhibits a distinct advantage as compared to the reported hydroarylation using expensive metal catalysts.[20a-c] Accordingly, the more easily accessible propargylanilines are considered starting materials for synthesizing the desired annulation products in one pot without the isolation of triazoles.

Furthermore, while monitoring the progress of the reaction on a thin-layer chromatography (TLC) chip under a UV lamp, the DQIs thus obtained exhibited bright emission. The quinoline fluorescence method had been employed for quantitatively monitoring histochemically reactive zinc in the brain[21] and for tracking zinc ions in living cells.[22a-b] As compared to that in quinolines, surprisingly, the deficiency of aromaticity and the short conjugation length of DQIs can result in strong emission from visible blue-green to yellow fluorescence with fluorescent quantum yields up to 66%. Details of fluorescence properties in DQIs were discussed in terms of the structure-oriented effects.

Results and Discussion

Optimization of conditions for Cu(I)-catalyzed annulation. The Cu(I)-catalyzed reaction is expected to trigger the intramolecular annulation of *N*-propargylanilines, thereby DQIs. According to a previous study,[23] *N,N*-disubstituted propargylanilines were directly transformed into acrylamidines in the presence of CuCl and triethylamine, indicated as **3a'** in Table 1. For the elegant synthesis of a desired DQI, the ketenimine intermediate generated *in situ* should be attacked by the benzene π-electrons instead of the non-bonding electrons of nitrogen, resulting in the formation of acrylamidines. For preventing the formation of undesired acrylamidines, different Cu(I) complexes, solvents, and reaction temperatures were carefully screened using **2a** as the model substrate. The synthesis of compound **2** from mono-substituted *N*-propargyl aniline **1** is included in the Supporting Information. In the presence of a catalytic amount of copper iodide and potassium carbonate (K_2CO_3), **2a** was treated with tosyl azide in anhydrous dichloromethane (DCM) at room temperature for 12 h, affording acrylamidine **3a'** (35%) along with a trace amount of desired compound **3a** (Table 1, entry 1).

Table 1. Optimization of conditions

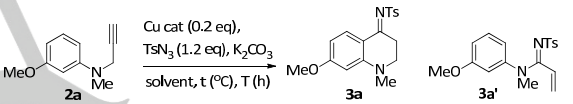

Entry	Catalyst	K_2CO_3 (eq)	Solvent	Temperature	Time	3a (%)	3a'(%)
1	CuI	1.5	DCM	rt	12	trace	35
2[a]	CuI	1.5	DMF	rt	12	—	—
3[b]	CuI	1.5	CH_3CN	rt	12	4	23
4[c]	CuBr	1.5	DCM	rt	30	7	30
5	CuCl	1.5	CH_3CN	rt	10	32	40
6[d]	CuCl	1.5	DCM	rt	12	54	11
7	CuCl	1.5	DCM	reflux	12	60	13
8[e]	CuCl	5.0	DCM	rt	12	63	—
9	CuCl	5.0	DCM	reflux	12	73	—

a)Formation of multiple spots; b)Recovered **2a** (30%); c) Triazole obtained (28%); d)Triazole obtained (18%); e)Triazole obtained (14%)

In *N,N*-dimethylacetamide (DMF) as the solvent, multiple spots were observed, but **3a** was not isolated (entry 2). Moreover, using acetonitrile (ACN) as the solvent, **3a** was obtained in only 4% yield (entry 3). Both copper bromide (CuBr) and copper chloride (CuCl) were also employed in this transformation in ACN and DCM. The use of CuCl in DCM afforded **3a** in 54% as the major product, along with minor acrylamidine **3a'** (11%; entry 6). According to a reported mechanistic study,[24] base additives and reaction temperature are factors important for controlling product distribution, thus for suppressing the formation of the undesired **3a'**. Hence, 5 equivalents of K_2CO_3 afforded the desired **3a** in 63%, with the unreacted intermediate triazole in 14%, without the formation of **3a'** (Table 1, entry 8). For enhancing annulations without forming undesired acrylamidines, 5 equivalents of K_2CO_3 under mild heating at 40°C were used, exclusively affording **3a** in 73% yield (Table 1, entry 9).

Scheme 2 shows the reaction mechanism, which was rationalized by two competing pathways. Tosyl triazole intermediate I could be prepared by treating *N*-propargylaniline with tosyl azide and the Cu(I) catalyst, which was in equilibrium with the α-imino diazo intermediate.

By a Wolff-type 1,2-rearrangement, highly reactive sulfonyl ketenimine II was obtained with the release of nitrogen gas[24], which then permitted intramolecular cyclization by phenyl π-electrons to form annulated intermediate IV. Then, the subsequent recovery of aromaticity and tautomerization afforded **3a** as the desired DQI, shown in Scheme 2 (path a).

Scheme 2. Proposed divergent pathways for the formation of cyclized **3a** and acrylamidine **3a'**

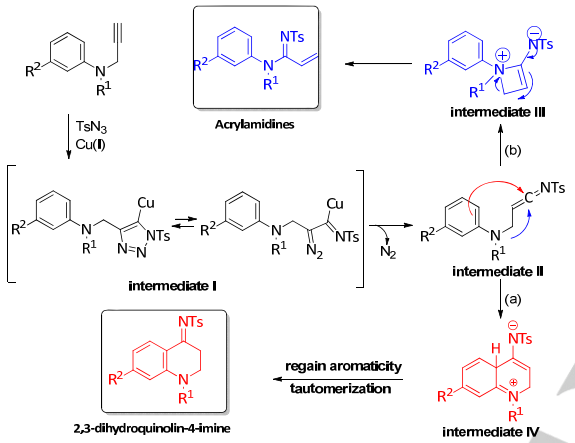

Alternatively, ketenimine II could be attacked by a tethered nitrogen nucleophile, forming 4-membered-ring intermediate III, followed by sequential rearrangement to afford acrylamidine **3a'**, as shown in path b.[23] Apparently, the desired annulation products are converted from the thermodynamically stable 6-membered-ring IV instead of the kinetically favored 4-membered-ring intermediate III, and the increasing reaction temperature could reasonably facilitate the formation of the desired cyclized product over the acrylamidine side products.

Expansion of substrate scope. Under the optimal reaction conditions, the substrate scope with respect to the *N*-substituents of **1** was carefully investigated (Table 2). Reactions with substrates **2b–2h** substituted with EDGs, such as alkyl groups and benzyl groups, proceeded smoothly, affording the corresponding products **3b–3h**, respectively, in good yields (63–88%), and only in case of the propyl substituent, the triazole intermediate was isolated as a byproduct **3g"** (14%).

However, reactions in which the tethered nitrogen of the substrates was protected by electron-withdrawing groups (EWGs) benzoyl group (R^1 = Bz) and tosyl group (R^1 = Ts), or without protecting groups (R^1 = H), multiple products were formed, except the desired products. (**3i** in Table 2) EWGs can destabilize the α-imino diazo and ketenimine intermediates, thereby resulting in decomposition. As the methoxy substituent at the meta position is thought to contribute to the resonance effect for facilitating annulation, the undesired acrylamidine **3j'** was exclusively obtained in 69% yield, which relocates the methoxy group from meta position to para position.

Table 2: Substrate scope with different substituents on the R^1 position.

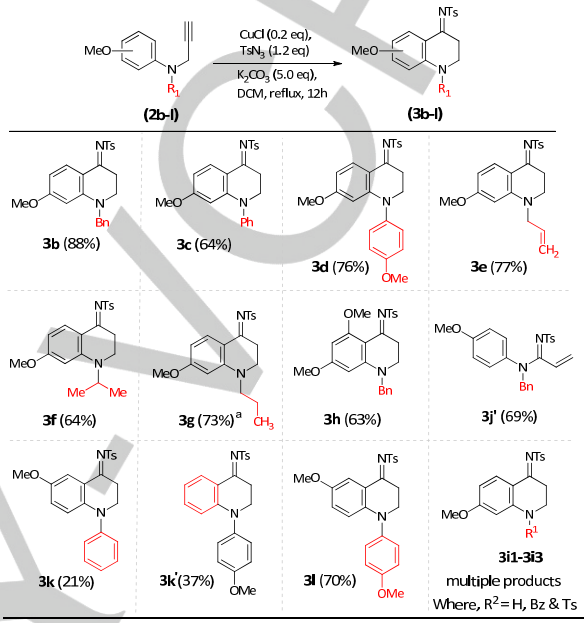

a) Compound **3g''** : 14%

Surprisingly, by changing the N-substituent to the phenyl group **2k** instead of the benzyl group, two annulation regioisomers **3k** and **3k'** were isolated in 21% and 37% yields, respectively. The introduction of the phenyl group on the nitrogen atom is believed to delocalize the non-bonding electrons, thereby resulting in annulation but not a nitrogen-directed nucleophilic attack. The substitution of 4-anisole in **2l** increased steric hindrance for avoiding the formation of acrylamidine and successful formation of the annulation product **3l** in 70% yield. Based on these results, the resonance effect due to the methoxy substituent at the para position can increase the electron density on the nitrogen atom and promote pathway b, as shown in Scheme 2. For efficiently controlling the formation of the desired annulation product with specific regioselectivity, the electronic and steric properties of the *N*-substituents (R^1) and the R^2 substituents on the phenyl ring are crucial, so as to prevent attack on the ketenimine intermediate to form acrylamidine and forming the desired annulation product.

The applicability of this method was further discussed for substrates by varying the R^2 substituents (**2m–2z**) and maintaining the R^1 substituent as the benzyl group. The replacement of the methoxy group with other substituents produced a number of substrates (**2m–z**, Table 3), which were subjected to the optimal reaction conditions. The electronic nature of the *meta* substituent on the benzene ring with either EDGs (**2m–u**) or EWGs (**2w–y**) resulted in the formation of products in moderate-to-good yields (47–87%).

As compared to the reported thermal condition,[10] Cu(I)-catalyzed annulation overcame the limitation of substrate scope, particularly for halo substituents (**2w** and **2x**) as well as the trifluoromethyl substituent (**2y**). Nevertheless, the introduction of a strong electron-withdrawing nitro substituent (**2z**) only formed acrylamidine (**3z'**, 72%). The nucleophilicity of the π-electrons is considerably reduced by the strong electron-withdrawing property of the nitro group, subsequently deactivating cyclization. In addition, the benzene ring without any substituent (**2v**) afforded the desired cyclized product in 80% yield, along with 8% acrylamidine as the byproduct (**3v** and **3v'**, respectively; Table 3).

Table 3: Substrate scope with different R^2 groups on the benzene ring

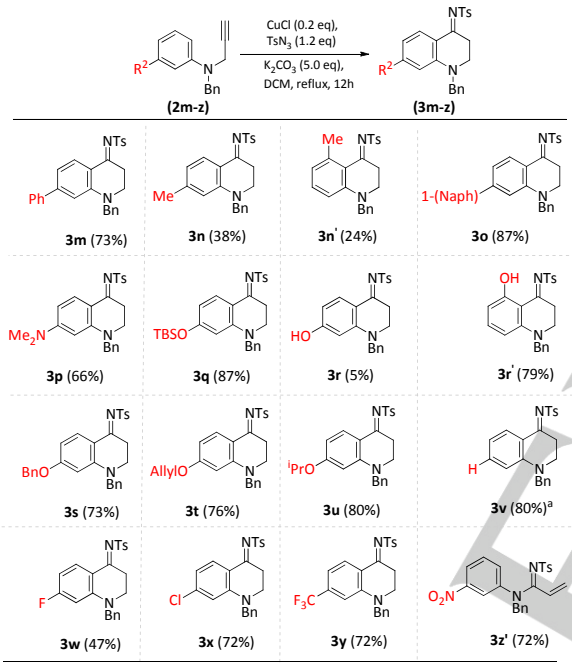

a) Compound **3v'** : 8%

Interestingly, 3-methyl substituent **2n** afforded two cyclized isomers, one cyclized at the C-6 of benzene (**3n**, 38%) and the other cyclized at the C-2 (**3n'**, 24%) position. Substrate **2r** with the hydroxyl group at the meta position afforded annulation product **3r'** at the C-2 position (79% yield) instead of the C-6-directed annulation product, along with a trace of desired cyclization product **3r** in 5% yield. Such regioselectivity is attributed to the fact that intramolecular hydrogen bonding between the hydroxyl and imine groups can direct annulation. The ORTEP diagram (Figure S1) of **3r'** shown in the Supporting Information also supports this conclusion.

Synthetic applications of 2,3-dihydroquinolin-4-imines. Furthermore, for extending the functionality of the DQIs obtained by this method, the *N*-sulfonylimine group of **3b** was transformed into other functional groups. In Scheme 3 (path a), the hydrolysis of sulfonyl imine using mild conditions, i.e., K_2CO_3 and MeOH, efficiently afforded 2,3-dihydro-4-quinolone **4b** in 74% yield, which is an important structural motif in several natural products; it also exhibits important biological activities.[25] Similarly, imine reduction in the cyclized product with sodium borohydride afforded amine **5b** in 83% yield, which is also a vital structural core unit in medicinal chemistry.[26]

Scheme 3: Synthetic utility

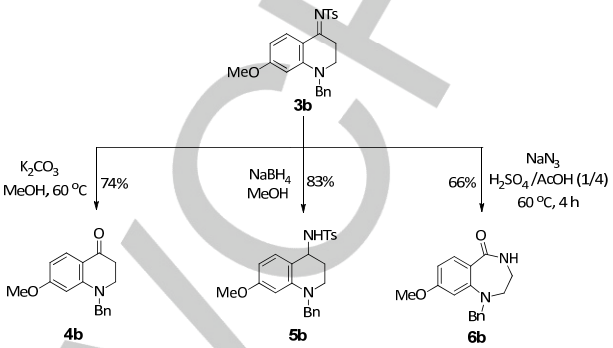

The creation of the amine and keto functionalities from the imine allows for further functionalization by various conjugation methods like Schiff base formation and amide bond formation. Importantly, the synthesis of tetrahydrobenzodiazepin-5-one via the Schmidt rearrangement of **3b** was also performed by the treatment of sodium azide under acidic conditions, affording synthetically valuable ring-expansion compound **6b** in 66% yield.[27] The methodology developed herein can be employed for the construction of not only various quinolone analogs but also alkaloids.

Table 4. Spectroscopic properties of fluorophores

Entry	Compound	λ_{abs}[a] (nm)	λ_{em}[b] (nm)	Φ_F (%)
1	**3a**	409	507	46
2	**3b**	409	500	28
3	**3c**	410	551	9
4	**3d**	411	505	-[c]
5	**3e**	409	501	35
6	**3f**	416	512	59
7	**3g**	417	509	63
8	**3h**	394	499	1
9	**3k**	460	-	-
10	**3k$_i$**	422	515	-[c]
11	**3l**	460	-	-
12	**3m**	434	527	60
13	**3n**	424	522	66
14	**3n'**	424	528	6
15	**3o**	422	549	64
16	**3p**	410	501	27
17	**3q**	411	501	43
18	**3r**	405	495	25
19	**3r$_i$**	447	510	-[c]
20	**3s**	409	500	36
21	**3t**	425	539	34
22	**3u**	409	500	42
23	**3v**	425	541	62
24	**3w**	411	499	19
25	**3x**	421	510	29
26	**3y**	428	538	37

a)Absorption maximum. b) Emission maximum. c)Fluorescence is too weak to be considered significant.

Photophysical properties of 2,3-dihydroquinolin-4-imines. Quinoline and its analogs are ideal fluorescent cores for metal ion sensors. However, the photophysical properties of quinolone and its reduced form, 2,3-dihydroxyquinolone are never addressed. To our surprise, during the analysis of the transformation proposed herein, the obtained DQIs exhibited

bright emission under a handy UV lamp on TLC chips. The development of small-molecule fluorescent probes accelerates the understanding of pathological and psychological roles of biomolecules in their native environments.[28a-b] To this end, the simple and easily modified structures of DQIs might potentially be a new series of molecular fluorophores with tunable photophysical properties. As this synthetic method was well established, various DQIs can be elegantly synthesized, and their photophysical properties were characterized.

For this purpose, the absorption and emission maxima along with fluorescent quantum yields of **3a–3y** were carefully measured; they are summarized in Table 4. The DQI fluorophores exhibited wavelengths of absorption maximum (λ_{max}) in the range of 394–460 nm, with emission maxima from 495 to 549 nm, resulting in blue-green to yellow fluorescence. The unexpectedly bathochromically shifted absorption is most probably resulting from intramolecular charge transfer from amino functionality to *N*-sulfonylimido group. Remarkably, the R^2 substituents, consisting of π-donating groups such as amino group (**3p**), alkoxy groups (**3q**, **3r**, **3s**, **3u**,), and fluoro group (**3w**), exhibited λ_{max} values near 410 nm. In contrast, the presence of EWGs such as chloro (**3x**), trifluoromethyl (**3y**), as well as no substituent (**3v**), clearly exhibited a red shift in absorption near 425 nm. In the case of compound **3r'** the absorption in further shifted to 447 nm. The 5-hydroxy group of **3r'** may contribute to intramolecular hydrogen bonding with the sulfonimido group, thereby affecting the chemical structure during photoexcitation.

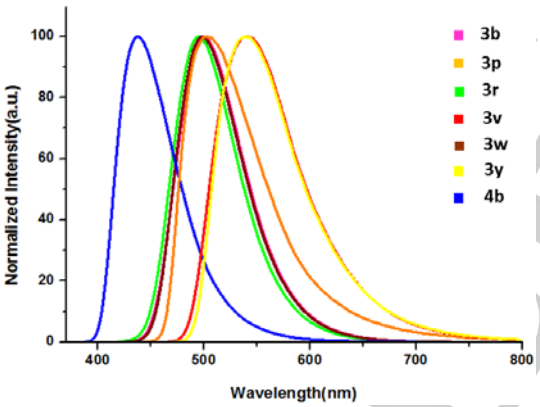

Figure 1. Fluorescence emission spectra of **3b**, **3p**, **3r**, **3v**, **3w**, **3y**, and **4b**.

The emission maximum of **3v** was observed at 541 nm. On the other hand, the substitution of π-donating groups at the position 7 of DQI, the blue-shift of emission was observed for the alkoxy groups (**3b**, **3d**, **3e**, **3f**, **3g**, **3h**, **3q**, **3u**, and **3w**), amino group (**3p**), and hydroxyl group (**3r** and **3r'**). The alkyl and phenyl substituents of the benzene ring, such as **3m** (λ_{em}: 527 nm) as well as **3n** and **3n'** (λ_{em}: 522 and 528 nm), slightly affected emission maxima. In contrast, the red-shift of emission was observed when an EWG (**3y**) or a naphthalenyl group (**3o**) was introduced at the position 7 of DQIs. As compared to **3v**, large Stokes shift of 127 nm and 110 nm were observed for **3o** and **3y**, respectively. Considering the *N*-substituents, alkyl substituents did not affect emission characteristics, but the phenyl substituent (**3c**) considerably shifted the emission maxima to 551 nm. Interestingly, the presence of the methoxy group in **3d** produced an emission at 505 nm, instead of λ_{em} at 515 nm in **3k'**.

Figure 1a shows the emission spectra of the representative molecules, which clearly indicates the shift depending on the chemical structures. The fluorescent quantum yields of **3a-3y** were determined in DCM by comparison with coumarin 153 as the standard.[29] Remarkably, an unusual high fluorescent quantum yield was observed up to 66% in **3n** along with several DQIs (**3g, 3m, 3o and 3v**) determined with more than 60%.

To provide a deeper understanding of the excited-state nature of DQI system, detailed DFT and TD-DFT calculations were performed for **3v**. The calculations reveal that only the first excited state falls in the energy range of visible light, whereas the remaining excited states are characterized by absorption wavelengths shorter than 300 nm. The wavelengths of S_0-S_1 vertical transitions with ground-state and excited-state geometries were calculated to be 405 and 539 nm, respectively, agreeing well with the experimental absorption and emission maxima (Figure 2). The S_0-S_1 electronic transition predominantly involves promotion of electron from HOMO to LUMO. Inspection of the pattern of HOMO and LUMO suggests that the electronic transition can be considered as π-π* transition with a certain degree of electron transfer from nitrogen in the ring to the N-sulfonylimido site. This can be confirmed by Mulliken population analysis, which reveals that the nitrogen atom in the ring becomes more positively charged and the *N*-sulfonylimido group, especially the C=N moiety, becomes more negatively charged upon electronic excitation (Figure S2).

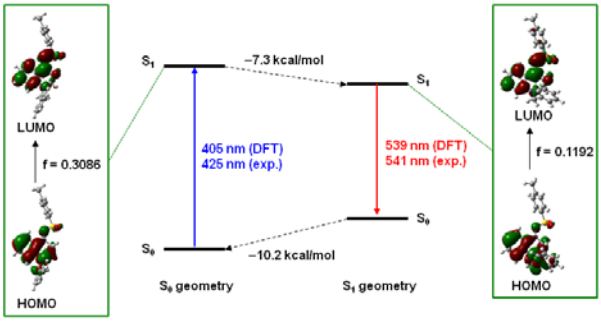

Figure 2. TD-DFT results for DQI **3v**, including absorption and emission wavelength, oscillator strength (f), and dominant configuration.

Subsequently, the variation of bond lengths caused by electronic excitation was estimated, as shown in Figure S3. The most apparent changes occur at C4–N bond and N–S bond that are elongated and shortened by 0.05 Å, respectively. These changes are consistent with the pattern of LUMO exhibiting significant anti-bonding character along the C4–N bond and bonding character along the N–S bond. In addition, non-negligible variations in bond lengths take place at the C2–C3, C5–C6, C7–C8, C8–C9, and N1–C9 bonds.

Population analysis for the HOMO and LUMO shown in Figure 3 indicates that while the former has significant distribution on the

C6 and C8 positions and negligible distribution on the C5 and C7 positions, the latter displays an opposite distribution on these positions. This feature provides an opportunity to individually adjust the energy of HOMO by substitution on C6 and C8 and adjust the energy of LUMO by substitution on C5 and C7, thereby tuning the HOMO-LUMO gap and modulating the absorption and emission wavelengths.

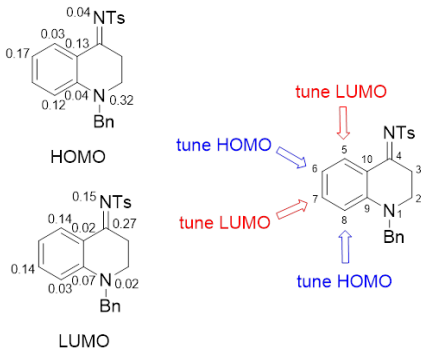

Figure3. Population analysis of HOMO and LUMO for **3v** (only fractional contributions larger than 0.01 are shown) and scheme for modulation of HOMO and LUMO energy.

The proposed strategy for modulating absorption and emission wavelengths of DQIs based on the DFT calculations has been further validated by experiments. From the data in Table 4, it can be seen that the absorption of **3c** is blue-shifted with respect to that of **3k**; in addition, the absorption and emission of **3d** are blue-shifted and the absorption of **3l** is red-shifted compared to unsubstituted **3k'**, respectively. This is because EDGs at C7 of **3c** and **3d** raise the LUMO energy level, leading to an increased HOMO-LUMO gap; EDGs at C6 of **3k** and **3l**, on the other hand, raise the HOMO energy level, reducing the HOMO-LUMO gap. Similar explanation can also be applied to the series of **3b**, **3n**, **3n'**, **3p**, **3q**, **3r**, **3s**, **3u**, **3w**, and **3x** in which EDGs are introduced at C5 or C7; all these compounds display the blue-shift of absorption and emission in comparison with the unsubstituted **3v** due to the rise of LUMO.

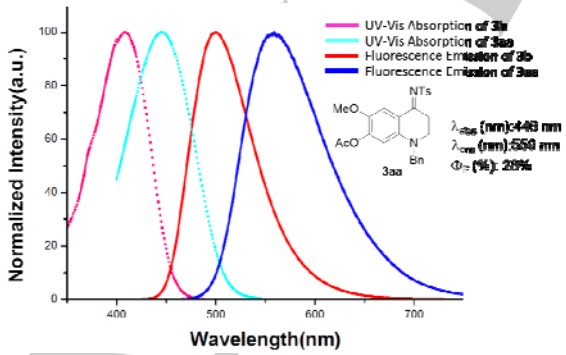

Figure 4. UV-Vis and fluorescence emission spectra of compound **3b** and **3aa**

To extend the fluorescence emission to longer wavelength, according to the DFT guideline, an EDG should be introduced at the position 6 of DQI to increase the energy level of HOMO along with an EWG at the position 7 of DQI to decrease the energy level of LUMO. This assumption has been validated by a tailored DQI **3aa**. In the **3aa** structure, a methoxy group was introduced at its position 6 as well as a weakly electro-withdrawing acetoxy group at the neighboring position 7. Compared to **3b**, which contains a methoxy group at the position 7, a significant red shift can be observed in both UV-VIS absorption and fluorescence emission spectra, as shown in Figure 4. The absorption wavelength shifts from 409 nm to 446 nm, indicating the reduction in energy gap between the HOMO and LUMO. Accordingly, a substantially increase in emission wavelength (up to 59 nm) is observed. The fluorescence emission of **3aa** is at 559 nm and its Stokes shift is 113 nm. The fluorescence quantum yield of **3aa** is determined as 28%.

To further understand the contribution of DQI structures in the corresponding photophysical properties, five control molecules **7**–**11** were synthesized and carefully characterized. First, the absorption of quinolin-4-imine **7**, the aromatic oxidized form of DQI, was determined at the wavelength of 361 nm, which could be mainly attributed its aromaticity instead of the charge transfer proposed in the DQI. Moreover, a blue fluorescence emission is observed at 456 nm but the intensity is too weak to be quantitatively analyzed. (Entry 1, Table 5) When oxygen atom replaces the nitrogen atom in the structure of DQI, the weaker charge transfer ability of oxygen atom reduces the absorption wavelength to 340 nm and the molecule shows no fluorescence under irradiation (control molecule **8**, Entry 2).

Table 5. Spectroscopic properties of control molecules

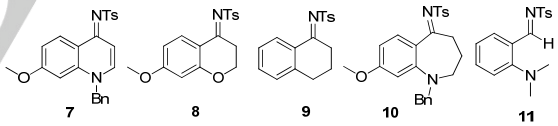

Entry	Compound	λ_{abs}[a] (nm)	λ_{em}[b] (nm)	Φ_F (%)
1	**7**	361	456	-[c]
2	**8**	340	-	-
3	**9**	278	-	-
4	**10**	390	481	-
5	**11**	401	551	5

a)Absorption maximum. b)Emission maximum. c)Fluorescence quantum yield is too weak to be determined. (λex:370 nm)

The carbon-linked analogue, 3,4-dihydronaphthalenimine **9**, shows no charge transfer and therefore, absorbs at 278 nm due to the benzylimine moiety.(Entry 3) For compound **10**, a seven-membered ring analogue of DQI, in which the charge transfer system is present but the ring size is larger, the absorption wavelength was determined to be 390 nm and it provides a very weak fluorescence at 481 nm.(Entry 4) The charge-transfer process is still available in this molecule, but with poor efficiency due to the greater flexibility of the bigger ring. Very importantly, an open-ring molecule **11** was synthesized, having a structure similar to **3v** but disconnects the fused cyclohexanimine. Notably,

the absorption of **11** at 401 nm, which is close to the absorption range of DQIs indicates that the 2-iminaniline moiety solely contributes to the intramolecular charge transfer process.
Furthermore, the emission λ_{max} of **11** was observed at 551 nm and its fluorescence quantum yield was determined to be 5%. Compared to DQI **3v**, the emission λ_{max} considerably shifts from 541 nm to 551 nm and the fluorescence quantum yield is reduced from 62% to 5%. This red-shift of emission and the loss in fluorescence quantum yield can be rationalized by the external relaxation process of **11** through internal rotation or a twisted intramolecular charge transfer (TICT) state with rapid rotations of the flexible open-chain framework. The relaxation process may also contribute to the reduction in fluorescence quantum yield. Therefore, the unique structure of DQIs with strong charge transfer motif, as well as the rigid ring structure, makes them new types of organic fluorophores with strong and modulable fluorescence.

Conclusions

In summary, 2,3-dihydroquinolin-4-imines (DQIs) were successfully synthesized by Cu(I)-catalyzed annulation, and were easily converted to 2,3-dihydroquinolones and various heterocyclic molecules. This synthetic strategy used easily available starting materials, *N*-substituted propargylanilines, which allows for the rapid expansion of substrate scope and accelerates the formation of a series of DQIs and molecular libraries of their analogs. The obtained DQIs exhibited unexpected photophysical properties with fluorescence quantum yields up to 66%. With the introduction of appropriate substituents, the emission wavelength of DQIs could be modulated from 495 nm to 559 nm to present corresponding blue-green to yellow color. The strong absorption of DQIs is due to the intramolecular charge-transfer process that may induce instantaneous change in the dipole moment. The development of similar donor-acceptor or energy transfer dyes attracts many attentions in the studies of material science and biological imaging.[30,31] A variety of DQIs synthesized in this research promise to emerge as a new class of environment-sensitive fluorophores with modulable fluorescence wavelengths. To understand the details of these structure-based DQI fluorophores, DFT calculations were performed and a reasonable design of DQI structures was obtained for specific photophysical properties. The tailored DQI 3aa was synthesized and showed a considerable emission red shift as expected. In this research, an efficient Cu(I)-catalyzed synthesis of DQIs has been proposed with wide substrate scopes and the obtained DQIs present enhanced fluorescent quantum yields with modulable emission wavelengths. The unique photophysical property of DQIs makes them important for the study of biosensing and bioimaging applications.

Experimental Section

All reactions were performed under an atmosphere of nitrogen and the workups were carried out in air. All the solvents used for the condition optimization were dried using reported procedures. Unless noted, all materials were purchased from commercial suppliers and used as received. Tosylazide was prepared in house using conventional procedure. Cuprisorb resin was purchased from Seachem Laboratory and dried in high vacuum before used. ^{1}H &^{13}C NMR spectra were recorded on BrukerUltrasheild™ 300 & 75 MHz spectrometer respectively. NMR data are reported as follows: chemical shift, multiplicity (s = singlet, d = doublet, t = triplet, q = quartet, m = multiplet), coupling constants (Hz). Solvent Residual peaks calibrations: for ^{1}H NMR: $CDCl_3$: 7.2600 ppm. For ^{13}C NMR: $CDCl_3$: 77.23 ppm. Melting Points of the products were calculated in open capillary tubes using Fargo Melting Point Apparatus MP-2D. Infra-Red spectra were recorded using Perkin Elmer 100 FTIR Spectrometer. High Resolution Mass Spectra (HRMS) were performed on an Electronspray Ionization Time-of-Flight (ESI-TOF), Fast Atom Bombardment (FAB), Electron Ionization (EI), and Atmospheric-pressure chemical ionization Time-of-Flight (APCI-TOF) mass spectrometer. Flash chromatography was performed using silica gel (43-60 mm, Merck).

Representative procedure for the synthesis of 3a-3h, 3k-3y:
Preparation of *N*-(1-benzyl-7-methoxy-2,3-dihydroquinolin-4(1*H*)-ylidene)-4-methyl benzenesulfonamide (3b). To a stirred solution of *N*-benzyl-3-methoxy-*N*-(prop-2-yn-1-yl)aniline (100 mg, 0.397 mmol) in Dichloromethane (10 mL) was added potassium carbonate (273.9 mg, 1.985 mmol), copper (I) chloride (7.8 mg, 0.0794 mmol) and tosylazide (94 mg, 0.477 mmol) at room temperature under nitrogen atmosphere. The reaction mixture was refluxed over a period of 12 h. After TLC confirmed the completion of the reaction, the reaction mixture was allowed to cool to the room temperature, quencehed with saturated NH_4Cl solution (5 ml), diluted with DCM (20 mL) and washed with H_2O (2 x 10 mL). The mixture was then dried over anhydrous $MgSO_4$, filtered and concentrated under reduced pressure to afford the crude mixture and then purified by silicagel column chromatography to afford the desired product (**3b**) (147 mg, 88%) as a yellow solid.

Computational Methods. The hybrid functional PBE0 (i.e., PBE1PBE)[32] in combination with the 6-31+G* basis set were used in the present density functional theory (DFT) and time-dependent DFT (TD-DFT) calculations. In fact, three additional DFT functionals, CAM-B3LYP[33], M06-2X[34], and ωB97XD[35], have also been tested and it turned out that PBE0 possesses the best performance for reproducing the absorption wavelength for the present DQI system. It is well-known that conventional DFT methods fail to describe van der Waals dispersion forces. To remedy the deficiency, the D3 version of Grimme's dispersion correction[36] was added. The calculations were performed in the presence of dichloromethane solvent (ε = 8.93) treated by SMD continuum solvation model.[37] All calculations were accomplished by Gaussian 09 program.[38]

Quantum yield determination. The quantum yields were determined by comparing the integrated area of the corrected emission spectrum of Coumarin153 (φ =0.93 in ethyl acetate)[39]. All spectra were collected at room temperature. In general, emission spectra were obtained by exciting at 409 nm. The quantum yield can be calculated using the following equation: $\Phi = \Phi_R(m/m_R)(n^2/n^2R)$. Where Φ_R = quantum yield of Coumarin153, m = the slope of the line obtained from the plot of the integrated fluorescence intensity versus absorbance, m_R = the slope of the line obtained from the plot of the integrated fluorescence intensity versus absorbance of Coumarin153, n = the solvent refractive index,[40] n_R = the solvent refractive index of ethyl acetate.

Acknowledgements

This work is supported by grants from Ministry of Science and Technology (MOST104-2738-M-110-001-, MOST104-2113-M-110-001-, MOST104-2627-M-007-003- and 105-2627-M-007-001-) and National Sun Yat-sen University (04B39131 and 04B39132).

Keywords: Fluorescent probes •Fluorescence •Catalysis •Heterocycles •Annulation

[1] A. Gomtsyan. *Chem. Heterocycl. Compd.* **2012**, *48*, 7-10.
[2] a) M. I. Andersson, A. P. MacGowan, *J. Antimicrob. Chemother.* **2003**, *51,* 1-11. (b) S. Heeb, M. P. Fletcher, S. R. Chhabra, S. P. Diggle, P. Williams, M. C. Camara, *FEMS Microbiol. Rev.* **2011**, *35*, 247-274.
[3] S. Michel, F. Tillequin, *Stud. Nat. Prod. Chem.* **1997**, *20*, 789-815.
[4] J. Liu, Y. Wang, Y. Sun, D. Marshall, S. Miao, G. Tonn, P. Anders, J. Tocker, H. L. Tang, J. Medina, *J. Bioorg. Med. Chem. Lett.* **2009**, *19*, 6840-6844.
[5] S. -X. Zhang, J. Feng, S. -C. Kuo, A. Brossi, E. Hamel, A. Tropsha, K. -H. Lee, *J. Med. Chem.* **2000**, *43*, 167-176.
[6] a) A. L. Tökés, L. Szilágyi, *Synth. Commun.* **1987**, *17*, 1235-1245; b) A. L. Tökés, G. Litkei, L. Szilágyi, *Synth.Commun*. **1992**, *22*, 2433-2445; c) K. H. Kumar, D. Muralidharan, P. T. Perumal. *Synthesis,* **2004**, *1*, 63-68; d) R. S. Varma, R. K. Saini, *Synlett.* **1997**, 857-858; e) N. Ahmed, J. E. V. Lier, *Tetrahedron Lett.* **2006**, *47*, 2725-2729; f) N. Ahmed, J. E. V. Lier, *Tetrahedron Lett.* **2007**, *48*, 13-15.
[7] D. Solé, F. Mariani, I. Fernández, M. A. Sierra. *J. Org. Chem.* **2012**, *77*, 10272-10284.
[8] X. Liu, Y. Lu, *Org. Lett.* **2010**, *12*, 5592-5595.
[9] R. A. Bunce, J. E. Schammerhorn, *J. Heterocycl. Chem.* **2013**, *50*, 373-380.
[10] C. -H. Chou, Y. -Y. Chen, B. Rajagopal, H. -C. Tu, K. -L. Chen, S. -F. Wang, C. -F. Liang, Y. -C. Tyan, P. -C. Lin, *Chem. Asian J.* **2016**, *11*, 757-765.
[11] I. Bae, H. Han, S. Chang, *J. Am. Chem. Soc*. **2005**, *127*, 2038-2039.
[12] S. H. Kim, S. H. Park, J. H. Choi, S. Chang, *Chem. Asian J.* **2011**, *6*, 2618 -2634.
[13] G. Cheng, X. Cui, *Org. Lett.* **2013**, *7*, 1480-1483.
[14] L. Sun, Y. Zhu, P. Lu, Y. Wang, *Org. Lett.* **2013**, *15*, 5894-5897.
[15] Y. Xing, B. Cheng, J. Wang, P. Lu, Y. Wang, *Org. Lett.* **2014**, *16*, 4814-4817.
[16] E. J. Yoo, S. Chang, *Org. Lett.* **2008**, *10*, 1163-1166.
[17] S. Li, Y. Luo, J. Wu, *Org. Lett.* **2011**, *13*, 3190-3193.
[18] S.-L. Cui, J. Wang, Y.-G. Wang, *Org. Lett.* **2007**, *9*, 5023-5025.
[19] B. Rajagopal, Y. -Y. Chen, C. -C. Chen, X. -Y. Liu, H. -R. Wang, P. -C. Lin, *J. Org. Chem.* **2014**, *79*, 1254-1264.
[20] a) P. D. Mendoza, A. M. Echavarren, *Pure Appl. Chem.* **2010**, *82*, 801-820; b) T. Kitamura, *Eur. J. Org. Chem*. **2009**, 1111-1125; c) Y. Yamamoto, I. D. Gridnev, N. T. Patil, T. Jin, *Chem. Commun.* **2009**, 5075-5087.
[21] C. J. Frederickson, E. J. Kasarskis, D. Ringo, R. E. Frederickson, *J. Neurosci. Methods* **1987**, *20*, 91-103.
[22] a) L. Xue, G. Li, D. Zhu, Q. Liu, H. Jiang, *Inorg. Chem*. **2012**, *51*, 10842-10849; b) L. Xue, G. Li, C. Yu, H. Jiang, *Chem. Eur. J.* **2012,** *18*, 1050-1054.
[23] D. P. Chauhan, S. J. Varma, A. Vijeta, P. Banerjee, P. Talukdar, *Chem. Commun.* **2014**, *50*, 323-325.
[24] E. J. Yoo, M. Ahlquist, I. Bae, K. B. Sharpless, V. V. Fokin, S. Chang, *J. Org. Chem.* **2008**, *73*, 5520-5528.
[25] Y. Xia, Z. -Y. Yang, P. Xia, K. F. Bastow, Y. Tachibana,; S. C. Kuo, E. Hamel, T. Hackl, K. H. Lee, *J. Med. Chem.* **1998**, *41*, 1155-1162.
[26] V. Sridharan, P. A. Suryavanshi, J. C. Menendez, *Chem. Rev.* **2011**, *111*, 7157-7259.
[27] R. A. Tapia, C. Centella, *Synth.Commun.* **2004**, *34*, 2757-2766.
[28] a) L. Yuan, W. Lin, K. Zheng, L. He, W. Huang, *Chem. Soc. Rev.* **2013**, *42*, 622-661; b) J. Chan, S. C. Dodani, C. J. Chang, *Nat. Chem.* **2012**, *4,* 973-984.
[29] A. S. Klymchenko, V. G. Pivovarenko, A. P. Demchenko, *J. Phys. Chem. A.* **2003**, *107,* 4211-4216 .
[30] (a) K. E. Sapsford, L. Berti, I. L. Medintz, *Angew. Chem. Int. Ed.,* **2006**, *45*, 4562-4588. (b) M. A. Saeed, H. T. M. Le, O. Š. Miljanić, *Acc. Chem. Res.* **2014,** *47,* 2074-2083. (c) T. D. Kim, K. S. Lee, *Macromol. Rapid Commun.* **2015**, *36*, 943-958.
[31] (a) J. Luo, J. Zhang, *ACS Catal.* **2016,** *6,* 873−877. (b) J. J. Bergkamp, S. Decurtins, S.-X. Liu, *Chem, Soc. Rev.* **2015**, *44*, 863-874.
[32] C. Adamo, V. Barone, *J. Chem. Phys.* **1999**, *110*, 6158−6170.
[33] T. Yanai, D. Tew, N. Handy, *Chem. Phys. Lett.* **2004**, *393*, 51−57.
[34] Y. Zhao, D. G. Truhlar, *J. Chem. Phys.* **2006**, *126*, 194101.
[35] J. D. Chai, M. Head-Gordon, *Phys. Chem. Chem. Phys.* **2008**, *10*, 6615−6620.
[36] S. Grimme, J. Antony, S. Ehrlich, H. Krieg, *J. Chem. Phys*. **2010**, *132*, 154104.
[37] A. V. Marenich, C. J. Cramer, D. G. Truhlar, *J. Phys. Chem. B* **2009**, *113*, 6378−6396.
[38] M. J. Frisch, G. W. Trucks, H. B. Schlegel, G. E. Scuseria, M. A. Robb, J. R. Cheeseman, G. Scalmani, V. Barone, B. Mennucci, G. A. Petersson, et al. Gaussian 09, revision D.01; Gaussian, Inc.: Wallingford, CT, **2009**.
[39] G. Jones II, W. R. Jackson, C.-Y. Choi, W. R. Bergmark, *J. Phys. Chem.* **1985**, *89*, 294-300.
[40] Handbook of organic solvent properties, Ian M. Smallwood; Halsted Press; John Wdey & Sons Inc. **1996**.

10.1002/chem.201703998

WILEY-VCH

Entry for the Table of Contents (Please choose one layout)

Layout 1:

FULL PAPER

Text for Table of Contents

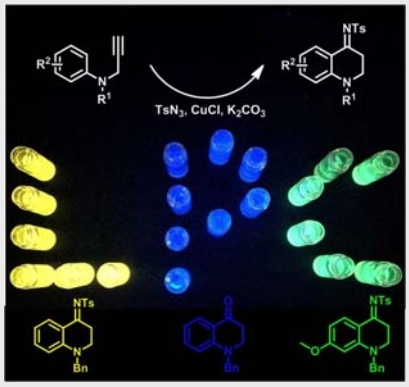

*Chih-Hung Chou,[+,a] Basker Rajagopal,[+,a] Chien-Fu Liang,[b] Kuan-Lin Chen,[a] Dun-Yuan Jin,[a] Hsing-Yin Chen,[*c] Hsiu-Chung Tu,[a] Yu-Ying Shen,[a] and Po-Chiao Lin[*a]*

Page No. – Page No.

Synthesis and Photophysical Characterization of 2,3-Dihydroquinolin-4-imines: New Fluorophores with Color-Tailored Emission